# Wavelet Analysis of the Pressure Signal in a Pulsating Heat Pipe

**Roberta Perna[1], Mauro Mameli[1], Alessandro Mariotti[2], Luca Pietrasanta[3], Marco Marengo[3], Sauro Filippeschi[1]**

[1] Department of Energy, Systems Land and Construction Engineering, University of Pisa, Largo L. Lazzarino, Pisa, Italy.
[2] Department of Civil and Industrial Engineering, University of Pisa, Via G. Caruso 8, 56122 Pisa, Italy
[3] Advanced Engineering Centre, School of Computing, Engineering and Mathematics, University of Brighton, Lewes Road, BN2 4GJ Brighton, UK
Corresponding author e-mail: c.robertaperna@gmail.com

**Abstract.** Thermally induced oscillations in two phase slug flow may largely affect the heat transfer in Pulsating Heat Pipes (PHPs). The prediction of the occurrence of flow instabilities and the definition of dominant frequencies, typical of different device operations, are still open issues. Their link is not known a priori, neither can be derived only from physical and analytical considerations. The studies available in the literature about different types of time-frequency analyses are very heterogenous and results are often discordant. In this work, the Wavelet Transform was used to characterize the signal in the frequency domain and identify the time interval in which these frequencies can be considered dominant. Data are collected varying the heat power input at the evaporator zone. During the slug-plug flow regime, we can estimate that the dominant frequency falls in the range $0.6 - 0.9\ Hz$. Clear trends show that the value of the dominant frequency increases with the heat load input. The understanding of the complex phenomena related to the thermally induced oscillations is essential for the development of reliable heat transfer models and robust design tools for Pulsating heat pipes which are presently limiting the diffusion of PHPs as thermal management devices.

## 1. Introduction

Thermally-induced oscillations in two phase confined slug flows largely affect the operation of heat transfer devices such as micro channel heat exchangers and wickless heat pipes, also known as Pulsating Heat Pipes (PHPs). In the first case these phenomena may lead to flow instabilities that are often detrimental for the device operation, causing a flow reversal to the inlet manifold [1] while, in the second case, they constitute the vary basic working principle [2]. For this reason, the frequency analysis of experimental data has been used in the literature to investigate the existence of dominant frequencies in the flow motion. The present work proposes to apply the wavelet transform, to the fluid local pressure signal of a PHP, to detect dominant frequencies and link them to the physical behaviour of the device. Frequency analysis on PHP have already been performed; Table 1 summarises the most relevant works available in literature. They can be grouped according to three factors: i) how they define the dominant frequency of a PHP signal; ii) the type of time-frequency technique they apply; iii) the experimental signal they use.

**Table 1: Literature review**

| *TIME-FREQUENCY TECHNIQUE* | *SIGNAL* | *AUTHORS* |
|---|---|---|
| Fast Fourier Transform (FFT) | $T_w$<br>$T_f$<br>$P_f$ | [3], [7], [8], [10]<br>[10], [11]<br>[4], [5], [12], [13] |
| Short Time Fourier Transform (STFT) | $T_w$ | [6] |
| Hilbert-Huang Transform (HHT) | $T_w$ | [6] |
| Time Strip Technique (TST) | $T_w$ | [9] |
| Wavelet Coefficient (WC) | $T_w$ | [7] |

Among the authors that have addressed PHPs, only a few have provided a definition of dominant frequency, while most researchers ignore this issue. Xu et al. [3] are the first to introduce the time-frequency analysis as a tool for modelling PHPs and they define the dominant frequency as the frequency corresponding to a peak of energy in the Power Spectrum. They performed the FFT on three wall temperatures signals at different heat loads. At 12 W, the dominant frequency value (0.1 Hz) is much smaller than those obtained at 25.6 W (0.46 Hz). The topic of "dominant" or "characteristic" pulsation frequencies is also investigated in Mameli et al. (2012) [4] and in Mameli et al. (2014) [5]. Both use the Fourier Transform analysis on the pressure signals at different heat input levels, but a dominant frequency is hardly recognisable in their results. This can imply that the FFT is not the right tool to detect dominant frequencies in a pseudo-steady flow. In this vein, Fairley et al. [6] describe the presence of energy peaks in the Power Spectrum as occurrence of intermittent high-energy oscillations in the PHP temperature signal. In their study, the Short-Time Fourier Transform (STFT) and Hilbert-Huang Transform (HHT) analyses are performed on the wall temperature and at different heat loads. The Hilbert-Huang energy spectrum shows intermittent oscillations with frequencies between $0.2\ Hz$ and $0.4\ Hz$. The results of the STFT are similar to those obtained with HHT, but the HHT's sharper time and frequency resolution makes some features of the energy spectra more evident. Overall, these pieces of work put sharp focus on the definition of dominant frequencies, but they only derive such definition from graphical results, as a frequency range.

On the application of the frequency analysis to different signals, the body of literature presents different perspectives on this point. The signal that is used the most is the wall temperature signal. To that signal, Zhao et al. [7] apply the FFT and the Wavelet Coefficient (WC). In the Fourier Power Spectrum, no dominant frequency is identified, when the original oscillating temperature signals are decomposed in a number of waveforms in terms of wave shape, frequency and amplitude are found. For the same signal, Chi et al. [8] use FT and find frequencies that fall in the range from $0.01$ to $0.05\ Hz$. In Spinato et al. [9] the 3D frequency spectra are computed for the local wall temperatures, as well as for the time-strip (or interval in the time domain) intensity at the same locations. Dominant frequencies are found to range from $0.6$ to $1.2\ Hz$. Monroe at al. [10] present the first work that compares the results obtained from an analysis on the wall temperature signal with those obtained on a fluid temperature signal. The results show that the frequencies of the fluid temperature fall in the range from $0.5$ to $4\ Hz$, while the wall temperature are absent, due to the thermal impedance of the tube wall and external TC attachment method. The FT is also applied by Ishii et al. [11] and in their work the transform considers the fluid temperature signal for different heat loads. For heat loads of $74.4$ to $238\ W$, the dominant frequencies are not visible in the power spectrum, while for $316\ W$ and $415\ W$ the peaks are identified around $2\ Hz$. As opposed to the above authors, others apply the Fourier Transform on the pressure signal. Among such works is Khandekar et al. [12], the frequency falls in the range from $0.4$ to $2.2\ Hz$. Also, in Takawalea et al. [13] the Fast Fourier Transform is applied on the pressure signals of PHP and dominant frequency can't be found but also indicates that the oscillation frequency in general increases with the heat input. The time delay is estimated from the autocorrelation function [13].

From the literature review and from physical considerations, it emerges that the useful information in terms of oscillation frequency is detectable only from the signal that are directly related to the fluid (fluid pressure and fluid temperature). In the present analysis, the Wavelet Transform (WT) technique is applied to all the three signals available (fluid and wall temperatures and the fluid pressure) to demonstrate that the fluid pressure is the best choice because this signal is not affected by the tube wall inertia or by intrinsic limits of thermocouples but directly linked to the internal fluid-dynamic. Moreover, the WT is chosen to overcome the limits of FT and STFT when a time-frequency localizations and multiresolution representations are required. Then the present work shows the wavelet analysis performed on the pressure signal of a real PHP tested in microgravity conditions during the $67^{th}$ ESA parabolic flight campaign, in order to avoid any pressure contribution related to buoyancy forces, with the following objectives: i) provide a quantitative definition of "Dominant Frequency" in PHPs; ii) assess whether there is a relationship between dominant frequencies and heat load input; iii) compare the dominant frequency of the signals, both at the evaporator and at the condenser.

## 2. Experimental set up

The PHP test cell consists of an annealed aluminium tube with an inner/outer diameter of 3/5 mm and it is described by Mameli et al. [14]. The tube is folded in a single loop staggered 3D configuration with fourteen turns in the evaporator zone as shown in Figure 1.

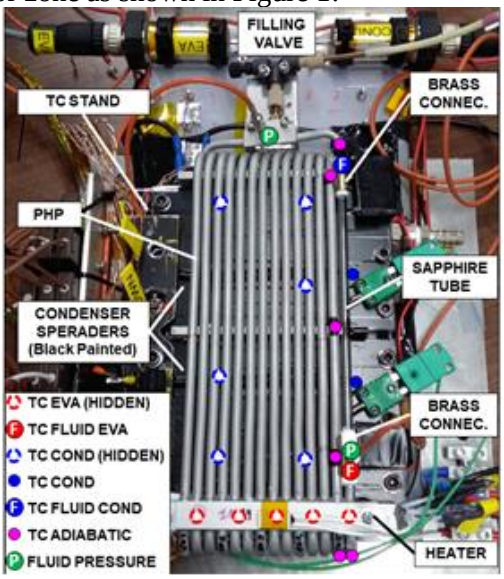


**Figure 1:** Actual test cell front view with pressure transducers location.

An aluminium T-junction allows to close the loop and hosts one pressure transducer (Keller® PAA-M5-HB, 1 bar abs, 0,2% FSO accuracy) along with the vacuum and filling port. Two brass connections allow to embed a sapphire tube insert and to host two K-type micro-thermocouples for the fluid temperature measurement, as well as one pressure transducer close to the evaporator section. Two ceramic ohmic heaters supply from a minimum of 18W to a maximum of 180W, corresponding to an average wall to fluid heat flux from 1.10 to 11.43 $W/cm^2$. The condenser zone is cooled down by means of eight Peltier cells and cold plate temperature control system. Five T-type thermocouples are located in between the spreader and the heater, one Pt-100 directly on the heater; eight on the tube external wall; six between the cold side of the Peltier cells and the condenser; two on the condenser spreader just behind the sapphire tube as shown in Figure 1. The device is partially filled with 22 ml of FC-72 (50% vol.). The test rig is then loaded on the Airbus A310 Zero-g and a total of 93 parabolic trajectories are performed over the three days of flight. The device is oriented in bottom heated mode (the main acceleration field in the flow path direction). During the thermal characterization, the device is heated up at the desired power level before the occurring of the microgravity period, and the power level is kept constant for the whole sequence of parabolae, the pressure signals are acquired at $200Hz$ and the fluid signals are acquired at $50Hz$.

## 3. Signal analysis methodology

The fluctuations of the pressure and temperature signals are characterized through techniques based on the continuous Wavelet Transform, WT. As described by Buresti et al. [15], a wavelet function can be any real or complex function $\psi(t) \in L^2$ that satisfies the following admissibility condition:

$$C_\psi = \int_{-\infty}^{+\infty} \left|\hat{\psi}(\omega)\right|^2 |\omega|^{-1} d\omega < \infty \tag{1}$$

where $\hat{\psi}(\omega)$ is the Fourier transform of $|\psi(t)|$. Indeed, to guarantee the reversibility of the transform, $C_\psi$ has to be a finite quantity and, in practice, this implies that $\psi(t)$ has zero mean value. Under this admissibility condition, the Wavelet Transform $W_x(a,\tau)$ can be defined the as follow:

$$W_x(a,\tau) = \frac{1}{\sqrt{a}} \int_{-\infty}^{+\infty} x(t) \psi^* \left(\frac{t-\tau}{a}\right) dt \tag{2}$$

where $a \in \Re^+$ is the scale dilation parameter and $\tau \in \Re$ is the translation parameter. In the present study, the complex Morlet wavelet $\psi(t) = e^{i\omega_0 t} e^{-t^2/2}$ is used, with a central frequency $\omega_0 = 2\pi$ in order to well-balance time and frequency resolutions. For the Morlet wavelet the frequencies, $f$ are related to the scales, $a$ by $f = \omega_0/(2\pi a)$, thus in this case we have $f = 1/a$. The wavelet power spectrum can be obtained from the integration in time, i.e. for each scale/frequency, the wavelet energy map, as:

$$P_{W_x}(a) = \frac{1}{C_\psi} |W_x(a,\tau)|^2 d\tau \tag{3}$$

In analogy to the signal analysis procedures used e.g. in [16], [17], in this paper Wavelet Transform is preferred to STFT for time-frequency analysis because it allowed us dynamically to increase frequency resolution at lower frequency values, whereas to increase time resolution at higher frequency values (in STFT a the frequency resolution is fixed). Moreover, compared to classical Fourier spectra, wavelet-based procedure allows to obtain smoother spectra and well defined from the mathematical point of view. The results in the following Section are reported in form of time-frequency energy maps $|W_x|^2$, (also called "scalograms") and wavelet spectra $P_{W_x}$. In the scalogram, the colour represents the energy value at the given time and frequency. The related spectrum will be used for the identification of the dominant frequencies.

## 4. Results and discussion

The Wavelet analysis is performed on the pressure ($P_f$), fluid temperature ($T_f$) and wall temperature ($T_w$) signals. The parameters considered for the measurements are: i) the heat load input $\dot{Q} = 68, 96, 134, 146\ W$; ii) the orientation BHM (Bottom Heated Mode); iii) the gravity field (microgravity). For the processing of the signals, an in-house-developed wavelet tool has been used, which was widely validated (see e.g.[16], [17]).

### *4.1. Definition of dominant frequency*

Given the wavelet power spectrum $\mathrm{P_{Wt}(f)}$, in the domain $\mathrm{Dom(P_{Wt})}$, the dominant frequency $(\mathrm{f_D})$ as the frequency at which the absolute maximum of the function is $\mathrm{P_{Wt}}(f)$ occur. Thus, from an analytical point of view:

$$\forall f \in \mathrm{Dom(P_{Wt})} \qquad \mathrm{P_{Wt}(f) < P_{Wt}(f_D)} \tag{7}$$

Since the wavelet power spectrum $\mathrm{P_{Wt}(f)}$ can present more than one peak, relative-maximum frequencies, also called characteristic frequencies, are also defined. The relative-maximum frequencies $\mathrm{f_C}$ exist if $\exists\ \mathrm{SubDom(P_{Wt})}$ with $f_D \notin \mathrm{SubDom(P_{Wt})}$ such that:

$$\forall f \in \mathrm{SubDom(P_{Wt})} \qquad \mathrm{P_{Wt}(f) \leq P_{Wt}(f_C)} \tag{8}$$

The dominant frequency ($f_D$) will be indicated in the Scalogram and in the Power Spectrum graphs as a black dashed line instead the characteristic frequency ($f_C$) as a black solid line (Figure 2). Once defined the dominant and the characteristic frequencies from the wavelet spectrum, it is possible to evaluate also their intermittency from the scalogram. Giving this definition is important because, it would allow to compare the results of different authors according to a unique and analytical definition.

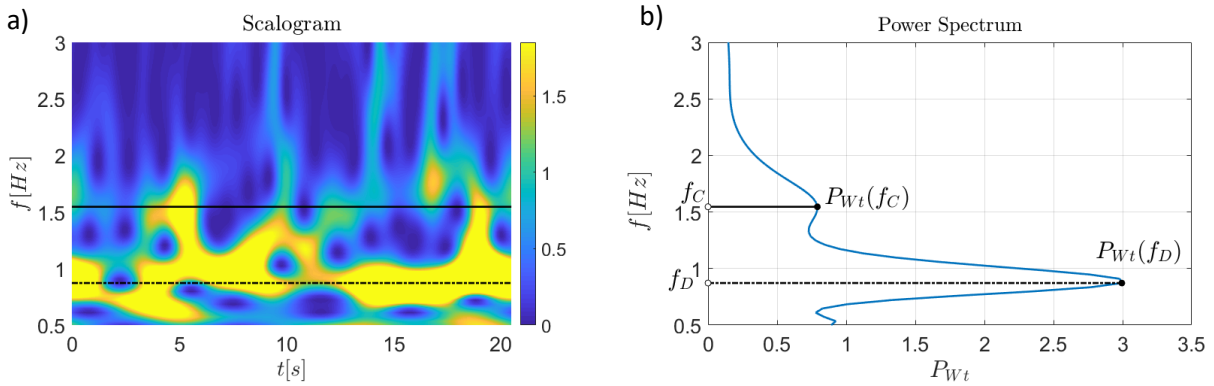


**Figure 2:** Example of Scalogram and Power Spectrum in which is identified the dominant frequency.

*4.2. Signal choice*

This section compare the results of a wavelet analysis which were obtained using different signals, fluid pressure ($P_f^e$), fluid temperature ($T_f^e$) and wall temperature ($T_w^e$) signals recorded in the evaporator zone during the same time interval. For the pressure signal, the acquisition frequency is $f_{Ac}^{P} = 200$ Hz and $N = 4096$ is chosen for an analysis with analysis time $t_{An} = 20.48$ s. Indeed, for the temperature signal, the acquisition frequency is $f_{Ac}^{T} = 50$ Hz and $N = 1024$ is chosen for an analysis with analysis time $t_{An} = 20.48$ s. For both signals, the $\mu g$ − level range is $-0.2 \leq g \leq 0.3$. Results are shown in Figure (3). These figures represent the Scalograms for each signal (Figure (3a) - (3b) - (3c)) and a Power Spectrum of all three signals in a unique graph (Figure (3d)), identifiable by the different colour of the plot ( $P_f^e$ , $T_f^e$ , $T_w^e$ respectively blue, green, black line). The fluid temperature signal appears to have the same dominant frequency as the pressure signal, with a lower energy content. The wall temperature signal, instead, does not show appreciable results in any frequency range, according to Monroe at al. [10], and this is due to the thermal impedance of the tube wall. The latter could depend on the fact the PHP envelope and its thermal inertia act as a low-pass filter RC circuit on the signal. For these reasons, this work analyses the pressure signal at the evaporator $P_f^e$ and condenser $P_f^c$ of the PHP.

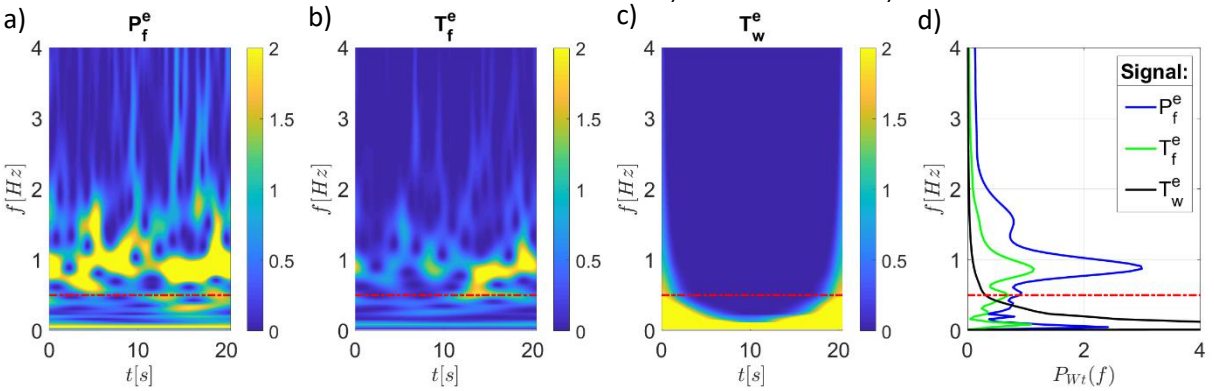


**Figure 3:** a) Wavelet Scalogram of the fluid pressure ($P_f^e$); b) Wavelet Scalogram of the fluid temperature ($T_f^e$); c) Wavelet Scalogram of the wall temperature ($T_w^e$); d) Power Spectrum of the fluid pressure ($P_f^e$) (blue line), the fluid temperature ($T_f^e$) (green line) and the wall temperature ($T_w^e$) (black line).

*4.3. Pressure signal wavelet analysis*

Currently, the detection of peaks in the time range can only rely on graphic methodologies, and it is thus a qualitative procedure, while the detection of peaks with respect to frequency can be based on numerical techniques. To ensure greater noise-free security, a frequency limit value $f \geq 0.5\ Hz$ is chosen. Above this value, the resulting values are not considered. Such a limit is indicated in the scalogram and power spectrum graphs as a red hatch. The Wavelet analysis for 17 parabolae representing the four power levels are analysed and compared. The Wavelet Scalogram and Power Spectrum of a signal are represented in Figure (4).

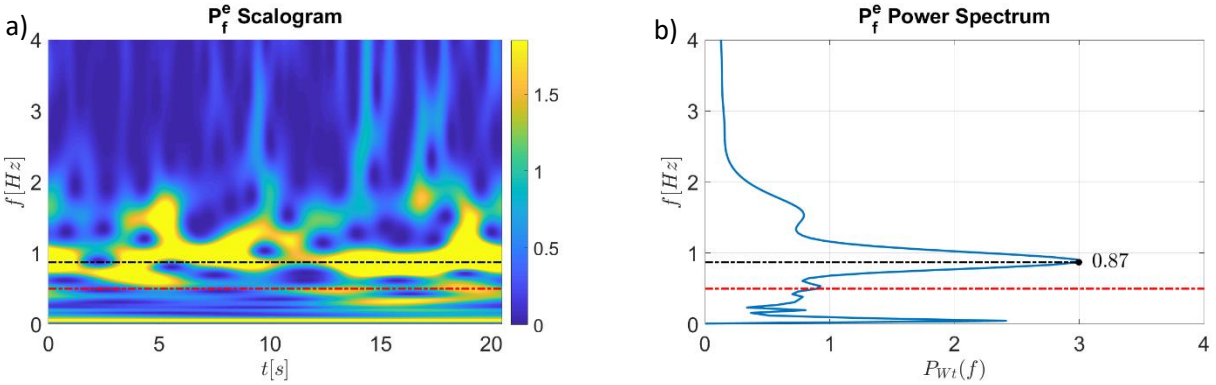


**Figure 4:** Wavelet Scalogram and related Power Spectrum of the fluid pressure signal ($P_f^e$).

**Table 2:** Power Spectrum results at the evaporator ($P_f^e$) and at the condenser ($P_f^c$).

| ***Day*** | ***p*** | $\dot{Q}$ ***[W]*** | $f_D^{P_f^e}$ ***[Hz]*** | $f_D^{P_f^c}$ ***[Hz]*** |
|---|---|---|---|---|
| I | 8 | 68 | 0,57 | 0,57 |
| I | 21 | 68 | 0,61 | 0,61 |
| I | 23 | 68 | 0,80 | 0,76 |
| I | 24 | 68 | 0,57 | 0,57 |
| I | 11 | 96 | 0,76 | 0,80 |
| I | 12 | 96 | 0,72 | 0,72 |
| I | 14 | 96 | 0,72 | 0,72 |
| I | 15 | 96 | 0,65 | 0,68 |
| I | 16 | 134 | 0,68 | 0,68 |
| I | 17 | 134 | 0,83 | 0,83 |
| I | 18 | 134 | 0,83 | 0,80 |
| I | 19 | 134 | 0,80 | 0,80 |
| II | 11 | 146 | 0,83 | 0,87 |
| II | 12 | 146 | 0,87 | 0,87 |
| II | 13 | 146 | 0,83 | 0,83 |
| II | 14 | 146 | 0,87 | 0,83 |
| II | 15 | 146 | 0,87 | 0,87 |

From these spectra, it is possible to analytically obtain information about the dominant frequency. Such values are listed in Table 2. The dominant frequency falls in the range 0.6 - 0.9 Hz. Clear trends are observed in Figure 5. They show that the value of the dominant frequency increases with increasing heat load input. In this paper state that the dominant frequency ($f_D$) is fairly proportional to the heat load input ($\dot{Q}$), as shown in Equation (9).

$$f_D \propto \dot{Q} \tag{9}$$

These graphs also illustrate the repeatability of our results, indicated by the black, grey and white points. For instance, as show in Table 2, at $\dot{Q} = 146\ W$, the results $f_D = 0.83\ Hz$ is repeated twice (grey points in Figure 5), while $f_D = 0.87\ Hz$ is repeated three times (black points in Figure 5).

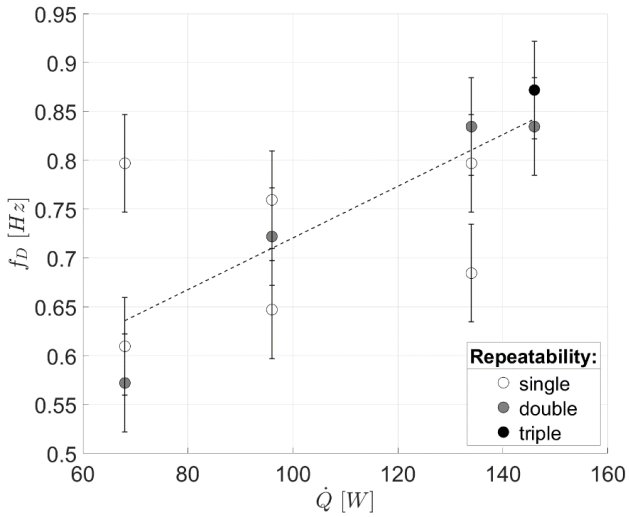


**Figure 5:** Dominant frequency trend with increasing heat load at the evaporator.

## 5. Conclusions

This paper describes the post-processing of data obtained from a Pulsating Heat Pipe (PHP) in microgravity conditions and with varying heat load input. The device is characterized by oscillating/pulsating thermally induced flow motion (slug/plug flow), which is intrinsically unsteady. The pressure and temperature of the PHP data is considered, recorded in microgravity condition, and a Wavelet analysis is conducted. The main results of this analysis are: i) the dominant frequency can be defined as the frequency relative to the maximum Power value, i.e. the signal peak in the Power Spectrum; ii) the wall temperature signal of the PHP cannot be used for Wavelet analysis, due to the thermal impedance of the tube wall; iii) the value of the dominant frequency of the pressure signals falls in the range 0.6-0.9 Hz and increases with increasing heat load input.

Overall, these results reveal the proportionality between dominant frequency and heat load input. Also, they emphasize the need to abide by a unique definition of dominant frequency of the PHP signal, which would make PHP studies comparable. Lastly, they suggest that heat transfer models that are currently used to characterize PHP oscillations in frequency domain are unreliable and insufficient in number. In this light, future work may try to develop mathematical models which accurately account for more and more parameters that characterise the operation of a PHP. In addition, they may investigate different types of relationships between the frequency and other device parameters, in order to improve our understanding of the operation PHP and to facilitate the implementation of effective heat transfer models.

## References

[1] Saha S.K., Celata G.P., "Instability in Flow Boiling in Microchannels", *SpringerBriefs in Applied Sciences and Technology*, 2016.

[2] Rao M., Lefèvre F., Czujko P., Khandekar S., Bonjour J.," Numerical and experimental investigations of thermally induced oscillating flow inside a capillary tube", *Int. J. of The. Sci.* 115, 29e42, 2017.

[3] J. L. Xu and X. M. Zhang, "Start-up and steady thermal oscillation of a pulsating heat pipe," *Heat and Mass Transfer/Waerme- und Stoffuebertragung*, vol. 41, no. 8, 2005.

[4] M. Mameli, S. Khandekar, and M. Marengo, "Are Dominant Oscillation Frequencies Always Present in Pulsating Heat Pipes ?," *Seventh International Symposium on TWO-PHASE SYSTEMS FOR GROUND AND SPACE APPLICATIONS, Beijing, China, September 17-21, 2012*, 2012.

[5] M. Mameli, M. Marengo, and S. Khandekar, "Local heat transfer measurement and thermo-fluid characterization of a pulsating heat pipe," *International Journal of Thermal Sciences*, vol. 75, 2014.

[6] J. D. Fairley, S. M. Thompson, and D. Anderson, "Time–frequency analysis of flat-plate oscillating heat pipes," *International Journal of Thermal Sciences*, vol. 91, 2015.

[7] N. Zhao, H. Ma, and X. Pan, "Wavelet Analysis of Oscillating Motions in an Oscillating Heat Pipe," 2012.

[8] R. G. Chi, W. S. Chung, and S. H. Rhi, "Thermal characteristics of an oscillating heat pipe cooling system for electric vehicle Li-ion batteries," *Energies*, vol. 11, no. 3, Feb. 2018.

[9] G. Spinato, N. Borhani, and J. R. Thome, "Understanding the self-sustained oscillating two-phase flow motion in a closed loop pulsating heat pipe," *Energy*, vol. 90, Oct. 2015.

[10] J. G. Monroe, Z. S. Aspin, J. D. Fairley, and S. M. Thompson, "Analysis and comparison of internal and external temperature measurements of a tubular oscillating heat pipe," *Experimental Thermal and Fluid Science*, vol. 84, 2017.

[11] K. Ishii and K. Fumoto, "Temperature visualization and investigation inside evaporator of pulsating heat pipe using temperature-sensitive paint," *Applied Thermal Engineering*, vol. 155, Jun. 2019.

[12] S. Khandekar, A. P. Gautam, and P. K. Sharma, "Multiple quasi-steady states in a closed loop pulsating heat pipe," *International Journal of Thermal Sciences*, vol. 48, no. 3, Mar. 2009.

[13] A. Takawale, S. Abraham, A. Sielaff, P. S. Mahapatra, A. Pattamatta, and P. Stephan, "A comparative study of flow regimes and thermal performance between flat plate pulsating heat pipe and capillary tube pulsating heat pipe," *Applied Thermal Engineering*, Feb. 2019.

[14] M. Mameli, A. Catarsi, D. Mangini, L. Pietrasanta, D. Fioriti, M. La Foresta, L. Caporale, M. Marengo, P. Di Marco, S. Filippeschi. "Large Diameter Pulsating Heat Pipe for Future Experiments on the International Space Station: Ground and Microgravity Thermal Response." *19th IHPC (International Heat Pipe Conference) and the 13th IHPS (International Heat Pipe Symposium)*, Pisa, Italy, 2018.

[15] G. Buresti, G. Lombardi, and J. Bellazzini, "On the analysis of fluctuating velocity signals through methods based on the wavelet and Hilbert transforms," *Chaos, Solitons and Fractals*, vol. 20, no. 1, 2004.

[16] A. Mariotti, G. Buresti, G. Gaggini, and M. v. Salvetti, "Separation control and drag reduction for boat-tailed axisymmetric bodies through contoured transverse grooves," *Journal of Fluid Mechanics*, vol. 832, 2017.

[17] A. Mariotti, "Axisymmetric bodies with fixed and free separation: Base-pressure and near-wake fluctuations," *Journal of Wind Engineering and Industrial Aerodynamics*, vol. 176, May 2018.